SURE 静岡大学学術リポジトリ
Shizuoka University REpository

Conformationally restricted 3′-modified ABA analogs for controlling ABA receptors

メタデータ	言語: English 出版者: 公開日: 2016-03-15 キーワード (Ja): キーワード (En): 作成者: Takeuchi, Jun, Ohnishi, Toshiyuki, Okamoto, Masanori, Todoroki, Yasushi メールアドレス: 所属:
URL	http://hdl.handle.net/10297/9330

Conformationally restricted 3′-modified ABA analogs for controlling ABA receptors

Jun Takeuchi,[a] Toshiyuki Ohnishi,[a,b] Masanori Okamoto[c] and Yasushi Todoroki*[a,b,d]

[a]*Graduate School of Agriculture, Shizuoka University, 836 Ohya, Suruga-ku, Shizuoka 422-8529, Japan.*

[b]*Reseach Institute of Green Science and Technology, Shizuoka University, 836 Ohya, Suruga-ku, Shizuoka 422-8529, Japan.*

[c]*Arid Land Research Center, Tottori University, 1390 Hamasaka, Tottori 680-0001, Japan.*

[d]*Graduate School of Science and Technology, Shizuoka University, 836 Ohya, Suruga-ku, Shizuoka 422-8529, Japan.*

**E-mail: todoroki.yasushi@shizuoka.ac.jp*

†Electronic supplementary information (ESI) available: Supplementary figures and NMR spectra of synthesized compounds. See DOI:

Abstract

The physiological functions of abscisic acid (ABA) are regulated by a signal transduction pathway involving cytosolic ABA receptors, which include 14 PYR/PYL/RCAR (PYL) proteins in *Arabidopsis*. The development of a PYL antagonist could be a valuable tool to improve our understanding of the roles of ABA. We previously developed 3′-hexylsulfanyl-ABA (AS6), whose *S*-hexyl chain blocks protein phosphatase 2C (PP2C) binding by steric hindrance. This finding not only validated our structure-based approach to the design of a PYL antagonist, but also provided a basis for the development of a more potent or subclass/subtype selective PYL antagonist. In the present study, we synthesized a conformationally restricted analog of AS6, namely propenyl-ABA with an *O*-butyl chain (PAO4), to improve the affinity for PYL proteins by reducing the entropic penalty for binding to the receptors. In seed germination assays, (+)-PAO4 was a slightly stronger antagonist than AS6 in *Arabidopsis* and a significantly stronger antagonist in lettuce. Analysis of the thermodynamic parameters associated with the formation of the *Arabidopsis* PYL-(+)-PAO4 complex revealed that (+)-PAO4 binds more strongly to PYL5 than AS6 owing to an entropic advantage. In PP2C assays, this enhancement effect was observed only for the monomeric PYL subclass containing PYL5, suggesting that (+)-PAO4 is more effective than AS6 in physiological events involving monomeric PYL proteins as ABA receptors.

Graphical abstract

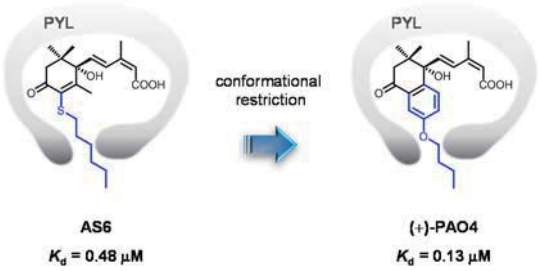

(+)-PAO4 is a conformationally restricted analog of the PYL antagonist AS6 that was synthesized to improve the affinity for PYL proteins by reducing the entropic penalty for binding to the receptors.

Introduction

The plant hormone abscisic acid (ABA, compound **1**) regulates various physiological processes, such as seed maturation and dormancy and stomatal closure, and it plays a role in the response to environmental stresses such as drought, cold and salinity[1,2]. The physiological functions of ABA are regulated by a signal transduction pathway mediated by the PYR/PYL/RCAR (PYL) family of receptors, which includes 14 PYL proteins in *Arabidopsis thaliana*[3,4]. Binding of ABA to PYL proteins induces a conformational change in a mobile loop (gate), triggering its closure and enabling the receptor to inhibit group-A protein phosphatases 2C (PP2Cs) such as HAB1, ABI1 and ABI2, which are negative regulators of ABA signaling[5–9]. A chemical compound capable of disrupting ABA signaling and homeostasis would be a valuable tool for dissecting the various roles of ABA[10].

Elucidation of the crystal structures of several PYL-ABA and PYL-ABA-PP2C complexes[11–13] has enabled the design of PYL antagonists based on its molecular structure. ABA binding induces a conformational change promoting the gate-closed form of PYL and intrudes deeply into the ligand binding domain, leading to the formation of a tightly packed pocket by PYL's residues; however, a small tunnel (referred to as the 3′-tunnel) was found on ABA's 3′-CH and its entrance lies on the PP2C binding interface. Based on this observation, in a previous study, we developed 3′-hexylsulfanyl-ABA (AS6, compound **2**), which contains an *S*-hexyl chain that protrudes through the tunnel and blocks PP2C binding by steric hindrance[14]. AS6 binds to PYL proteins with comparable affinity to ABA, and antagonizes ABA-mediated inhibition of PP2C in all 11 PYL proteins tested. These results validated our structure-based approach to the design of ABA antagonists.

Despite the potential value of AS6 for improving our understanding of the roles of ABA, the function of this inhibitor can be improved (i.e. increased potency) or transformed (e.g. subtype selective) through appropriate structural modifications. The 3′-*S*-hexyl chain of AS6 is a critical substituent for hindering the PYL-PP2C interaction. The crystal structure of the PYR1-AS6 complex indicates that to function as a PYL antagonist, the 3′-substituent of an ABA analog needs to be long enough to block PP2C binding and sufficiently thin to fit into

the 3′-tunnel without preventing the conformational change of PYL into the gate-closed form (ESI† Fig. 1). The *S*-hexyl chain meets both of these requirements; however, the high flexibility derived from its seven sp^3 atoms results in a loss of entropy and decreases the affinity for binding to PYL. Because the base (-S-CH_2-) of the chain is not located in the 3′-tunnel, but rather inside the pocket, it does not need to be thin to fit into the tunnel. Therefore, structural modification of this portion may decrease the flexibility of the chain without altering certain properties required for fitting into the tunnel to induce a conformational change in PYL. An increase in the rigidity of the chain may intensify the affinity for binding to PYL by decreasing the entropy loss associated with the formation of the complex. This conformational restriction strategy has been widely used in modern drug design to create potent and selective ligands[15,16]. Here, we tested whether this strategy is applicable to PYL proteins for the development of a more potent antagonist than AS6.

Results and discussion

Design and synthesis of new PYL antagonists: PAO*n* compounds

We selected a tetralone ABA analog (compound **3**), whose cyclohexenone ring is fused with a benzene ring, as a core for constructing a conformationally restricted PYL antagonist. Compound **3** is a biologically active ABA analog[17], suggesting that the addition of a benzene ring introduces a restricted portion, namely -CH=CH-, in place of the flexible -S-CH_2- of AS6 without interfering with the PYL conformational change (Fig. 1). An *O*-butyl group was selected for the residual C_5 chain portion to improve the efficacy of synthesis, and the new compound was designated as PAO4 [propenyl-ABA with *O*-butyl (4 carbons) chain, compound **4**]. A superposition of PAO4 and AS6 in the PYR1-AS6 complex (3WG8) indicated that the *O*-butyl chain of PAO4 was sufficiently long to protrude through the PYR1 surface (ESI† Fig. 2). Therefore, PAO4 was expected to inhibit PYL-PP2C interactions by the same mechanism as AS6. It may also be a stronger antagonist of the effect of ABA than AS6

because of its higher binding affinity for PYL proteins.

We synthesized six PAO*n* compounds (*n* = 1–6; Scheme 1) containing shorter and longer chains in addition to the C_4 chain to evaluate the effect of chain length on the agonist/antagonist properties of the compound. Racemic PAO*n* compounds were synthesized from commercially available 6-methoxy-1-tetralone (**5**) according to scheme 1[17,18]. The germinal methyl groups were introduced by treatment of compound **5** with methyl iodide in the presence of sodium hydride, yielding the dimethyl compound **6**. Compound **6** was refluxed with 48% hydrobromic acid to generate the phenolic compound **7**. The phenolic hydroxyl group was protected by a *tert*-butyldimethylsilyl group to yield compound **8**. The side chain was introduced by direct addition of (*Z*)-3-methyl-2-penten-4-yn-1-ol using *n*-butyllithium, generating the alcohol **9**. Reduction (generating compound **10**), oxidation (generating compound **11**) and esterification of **9** resulted in the formation of the ester **12**. Benzylic oxidation with pyridinium dichromate and *tert*-butyl hydroperoxide afforded ketone **13**, which was deprotected by potassium fluoride in tetraethylene glycol to yield compound **14**. Introduction of an alkyl chain by treatment of **14** with 1-iodoalkyl in the presence of potassium carbonate yielded racemic methyl esters, followed by basic hydrolysis of the esters to give (±)-PAO*n* (**15-20**). (±)-PAO4 and (±)-PAO1 were optically resolved by HPLC on a chiral column. The absolute configuration of optically pure PAO4 and PAO1 was determined by the circular dichroism exciton chirality method[19] (ESI† Fig. 3): both (+)-isomers have the *S*-configuration similarly to AS6 and naturally occurring ABA.

Biological activity of (+)-PAO4

The biological activity of (+)-PAO4 was examined using the *Arabidopsis* and lettuce seed germination assays, which rely on the inhibitory effect of ABA on germination. Here, PYL agonists inhibit seed germination and PYL antagonists relieve this inhibition in response to cotreatment with ABA. (+)-PAO4 did not inhibit *Arabidopsis* seed germination, and suppressed the ABA-induced inhibition with a slightly stronger effect than AS6 when used in combination with ABA (Fig. 2). In lettuce, (+)-PAO4 showed a significantly stronger

antagonistic activity than AS6 (Fig. 3). These results could be attributed to the stronger affinity of (+)-PAO4 for PYL compared to AS6. The difference between the effect of the compound in *Arabidopsis* and lettuce seeds could be related to structural differences between *Arabidopsis* and lettuce PYL proteins, although we cannot exclude the possibility that (+)-PAO4 may be less sensitive to metabolic inactivation in lettuce than in Arabidopsis. Further structural characterization of lettuce PYL proteins is necessary to confirm this hypothesis.

In the *Arabidopsis* assay, (−)-PAO4 was inactive, whereas the activity of racemic PAO4 was similar to that of the (+)-isomer (ESI† Fig. 4). This is reasonable because (−)-PAO4 should not be able to bind the ligand pocket of PYL proteins because of the steric hindrance of the *O*-butyl chain, as predicted by the model structure of the PYL-PAO4 complex. The remaining PAO*n* compounds were examined in a similar manner. For this purpose, we used the racemic forms of PAO*n* without optical resolution to investigate whether the PAO*n* compounds switch from agonistic to antagonistic according to the length of their *O*-alkyl chains. The racemic PAO*n* acted as an agonist when $n < 3$ and as an antagonist when $n \geq 3$ (ESI† Fig. 5). This chain length-dependent activity was similar to that of AS*n* compounds, suggesting that PAO*n* compounds function as agonist/antagonist of PYL through a mechanism similar to that of AS*n* compounds. In the case of (+)-PAO4, the *O*-butyl chain may protrude through the 3′-tunnel and prevent PP2C binding.

Comparison of the affinity of (+)-PAO4 and AS6 for binding to *Arabidopsis* PYL proteins

Arabidopsis PYL proteins are classified into two distinct subclasses according to their oligomeric state: PYR1 and PYL1–PYL3 form dimers in solution, whereas PYL4–PYL12 exist as monomers[20,21]. Isothermal titration calorimetry (ITC) was used to characterize (+)-PAO4 binding with monomeric receptors (PYL5 and PYL10), which simply associate with a ligand without dissociation of the receptor dimer. The K_d values and the thermodynamic constants, the change of enthalpy (ΔH), entropy ($-T\Delta S$) and free energy (ΔG) for PYL-(+)-PAO4 interactions are listed in Table 1. For the binding to PYL5, the affinity of

(+)-PAO4 (K_d = 0.13 μM) was 3-fold greater than that of AS6 (K_d = 0.48 μM). When compared with AS6, (+)-PAO4 binding was associated with a smaller negative enthalpy (ΔH = −6.7 kcal/mol and −9.7 kcal/mol for (+)-PAO4 and AS6, respectively). For the entropy change, AS6 exhibited a negative value, whereas (+)-PAO4 had a positive one. This may be attributed to the hydrophobic interaction on the phenyl moiety in addition to the reduction of the entropic penalty by conformational restriction. A different profile was obtained for the PYL10-(+)-PAO4 interaction, as the ΔH for (+)-PAO4 was more negative (−8.9 kcal/mol) than that for AS6 (−6.9 kcal/mol), whereas the $T\Delta S$ for (+)-PAO4 was lower than that for AS6. Consequently, (+)-PAO4 showed almost the same binding affinity as AS6. The enthalpy gain for the interaction of (+)-PAO4 with PYL10 compared with that observed for AS6 suggested the presence of additional interactions associated with the benzene ring of (+)-PAO4. A similar trend was observed for (+)-PAO1 binding to PYL5 and PYL10 (Table 1), suggesting that the effect of the benzene ring introduced into C2′-C3′ of ABA on binding to PYL may differ in each PYL subtype. (+)-PAO4 may be more effective than AS6 in physiological events dominated by PYL proteins with the PYL5-like character, whereas it may be as effective as AS6 in other processes.

Comparison of the effects of (+)-PAO4 and AS6 on different PYL subtypes

The subclass/subtype selective properties of (+)-PAO4 were compared with those of AS6 by assessing receptor-mediated PP2C inhibition using nine *Arabidopsis* PYL proteins (dimeric subclass: PYR1, PYL1–PYL3; monomeric subclass: PYL4–PYL6, PYL8, and PYL10) and HAB1 as PP2C. (+)-PAO4 exhibited a similar overall ligand profile to that of AS6. (+)-PAO4 showed weak inhibitory activity against HAB1 in the dimeric PYL subclass; its effect saturated at approximately 50% HAB1 inhibition with PYR1, which suggested that (+)-PAO4 acted as a weak partial agonist (Fig. 4a and b). This partial agonistic effect on the dimeric PYL subclass in the PP2C assay, which was also observed for AS6, was not detected in the *Arabidopsis* and lettuce seed germination assays. This weak inhibition of PP2C activity may be insufficient to activate ABA signaling or may only be detectable in an *in vitro* PP2C assay

system using an artificial, small substrate[14]. (+)-PAO4 had no effect on the monomeric PYL subclass except for PYL10, which was the only subclass in which (+)-PAO4 completely suppressed ABA-independent PP2C inhibition. When used in combination with ABA, (+)-PAO4 rescued HAB1 from ABA-induced inhibition for all the PYL proteins tested (Fig. 4c and d). This antagonistic activity was slightly lower for the dimeric PYL subclass and significantly greater for the monomeric PYL subclass than that of AS6 (discussed later).

We also evaluated the ligand profile of (+)-PAO1 against each PYL protein using the *in vitro* PP2C assay. The effect of (+)-PAO1 differed according to the subclass/subtype of PYL proteins (Fig. 4a and c), with a strong agonistic effect on dimeric PYR1 and PYL1–PYL3 and monomeric PYL4 and PYL5, and a strong antagonistic effect on monomeric PYL10. The effect on PYL6 and PYL8 was weak. This ligand profile was similar to that of AS2, as previously reported[14]. ABA analogs with a substituent at the 3′-position may be not effective ligands for certain monomeric PYL proteins. Conversely, the strong antagonistic effect of (+)-PAO1 on PYL10 is difficult to explain, because the *O*-methyl chain of (+)-PAO1 is estimated to be too short to directly interfere with binding to PP2C. The complex ligand profile of (+)-PAO1 could be explained by interactions between the 3′-substituent and the residues comprising the 3′-tunnel of PYL proteins. The only residue in the 3′-tunnel that differs among all the PYL proteins is located in the α3 helix that positions on ABA's 3′-ring CH in the PYL-ABA complex. This residue was identified as Val in PYR1 and PYL1–PYL3, Leu in PYL7–PYL10, and Ile in PYL4–PYL6 and PYL11–PYL13 (ESI† Fig. 7a). Based on the increasing bulkiness of the side chain from Leu to Ile to Val, the steric tolerance of the 3′-tunnel of the PYL proteins tested increased from dimeric PYR1 and PYL1–PYL3, to monomeric PYL4–PYL6, to monomeric PYL8 and PYL10. The agonistic profile of (+)-PAO1 depended on the steric tolerance in the 3′-tunnel of PYL proteins. Therefore, PYL proteins with lower steric tolerance, such as PYL8 and PYL10, may be unable to accommodate the 3′-substituent of (+)-PAO1 in the gate-closed form. However, if a PYL protein adopts the stable gate-opened form by accommodating a ligand, then this ligand should function as an antagonist, or more accurately an inverse agonist, by stabilizing the inactive form of the PYL

protein. This mechanism could explain the PYL10-(+)-PAO1 and PYL10-(+)-PAO4 interactions.

PYL10 can adopt the gate-closed form and inhibit PP2C even in the absence of ABA[21]. This was also observed in our PP2C assay, which showed that HAB1 activity in the presence of PYL10 was approximately 60% of that in the absence of PYL proteins (Fig. 4c). Because (+)-PAO1 and (+)-PAO4 reversed the ABA-independent PP2C inhibition of PYL10, binding of these ligands may have resulted in a transformation from the gate-closed form in the absence of ABA to the gate-opened form. The gate-closed form of PYL10 in the absence of ABA is stabilized by the unique residue at the N-terminal of the gate loop region[21]. In all PYL proteins except PYL10, this residue is Val, which makes a hydrophobic network with the C7′-C2′-C3′ region of the ABA and the α3 residue (Val, Ile, or Leu) to stabilize the gate-closed form. The corresponding residue in PYL10 is the bulkier Leu, which is present in both the gate loop and α3 helix. (+)-PAO1 and (+)-PAO4 may stabilize the gate-opened form of PYL10 by interacting with these two bulky Leu residues, which may facilitate the hydrophobic interaction between the α3 helix and the gate loop to induce the gate-closed form, even in the absence of ABA. The enthalpy gain observed in the ITC experiments testing (+)-PAO1 and (+)-PAO4 with PYL10 might be derived from the van der Waals or CH/π interaction between the benzene ring of these ligands and the Leu residues of PYL10, resulting in the stabilization of the complex with PYL10 in the gate-opened form (ESI† Fig. 7).

The steric tolerance of the 3′-tunnel of PYL proteins (except PYL10) may also have an effect on the antagonistic activity of (+)-PAO4 compared to that of AS6. The interaction of the 3′-*S*-hexyl chain of AS6 with the 3′-tunnel of PYL proteins should be tighter for the monomeric PYL subclass with α3 Ile or Leu than for the dimeric PYL proteins with α3 Val. Namely, the entropic penalty for AS6 binding should be greater for the monomeric PYL subclass. This could explain the higher antagonistic activity of (+)-PAO4 with a partially constrained 3′-chain than that of AS6 for the monomeric PYL subclass including PYL5 (Fig. 4c and d).

Comparison of the effects of (+)-PAO1 and ABA on physiological function

In phosphatase assays, (+)-PAO4 acted as an antagonist for all the PYL proteins tested, while (+)-PAO1 exhibited PYL subclass/subtype-selective agonistic activity: it activated PYR1 and PYL1–PYL6, but not PYL8 and PYL10. This suggests that (+)-PAO1 could be used as a chemical tool to examine the contributions of PYL subclasses/subtypes with specific physiological functions of ABA. To determine the practical value of the selective activation of PYL subtypes by (+)-PAO1 for the regulation of ABA-induced physiological responses, we tested the effect of (+)-PAO1 on two well-known ABA responses, namely seed germination and root growth. In *Arabidopsis* seed germination, where at least six members of the PYL family of proteins (PYR1, PYL1, PYL2, PYL4, PYL5 and PYL8) are involved in ABA signaling[22], (+)-PAO1 showed inhibitory activity with potency comparable to that of ABA (ESI† Fig. 8). However, (+)-PAO1 did not inhibit root growth with the same potency as ABA (ESI† Fig. 9), probably because (+)-PAO1 does not function as an agonist for PYL8 with a nonredundant role in root sensitivity to ABA[23]. These results suggested that (+)-PAO1 acts as a PYL subclass/subtype-selective agonist not only *in vitro* but also at the physiological level.

Conclusions

We synthesized (+)-PAO4 as a conformationally restricted analog of the previously developed PYL antagonist AS6 to improve its affinity for PYL proteins by reducing the entropic penalty on binding to the receptors. ITC experiments revealed that the affinity of (+)-PAO4 for PYL5 was 3-fold greater than that of AS6 owing to an entropic advantage. However, this enhancement effect was not observed for PYL10. The antagonistic effect of (+)-PAO4 on PP2C inhibition induced by a PYL-ABA complex was greater than that of AS6 only in the monomeric PYL subclass, including PYL5 and PYL10. This suggested that (+)-PAO4 is more effective than AS6 in physiological events in which the monomeric PYL subclass plays a major role, whereas it may be as effective as AS6 in other situations. (+)-PAO4 was a slightly stronger antagonist than AS6 in *Arabidopsis* seed germination assays, and a significantly

stronger antagonist in lettuce seed germination assays. The small difference in antagonistic activity between (+)-PAO4 and AS6 in *Arabidopsis* was consistent with the fact that the dimeric PYL subclass plays a key role in ABA signaling in *Arabidopsis*[24]. In lettuce, the monomeric PYL subclass may play an important role in ABA signaling, although lettuce PYL proteins have never been characterized. These results suggest that the conformational restriction strategy applied to AS6 is effective, although not dramatically, to develop a more potent PYL antagonist than AS6. The complex ligand profile of (+)-PAO1 suggests that 3′-modified ABA analogs are useful probes to elucidate the functional differences among ABA receptors and to manipulate the gate-closing mechanism of PYL proteins, in addition to its potential as a PYL subclass/subtype selective agonist/antagonist/inverse agonist.

Methods

General procedures

ABA was a gift from Dr. Y. Kamuro and Toray Industries Inc., Tokyo, Japan. ^{1}H NMR spectra were recorded with tetramethylsilane as the internal standard using JEOLJNM-EX270 (270 MHz) and JNM-LA500 (500 MHz) NMR spectrometers (JEOL Ltd., Tokyo, Japan). ^{13}C NMR and 2D-correlation NMR experiments were recorded using a JNM-LA500 (500 MHz) NMR spectrometer (JEOL Ltd.). All peak assignments refer to the numbering in structure **(+)-PAO4** (Fig. 1). High resolution mass spectra were obtained with a JEOL JMS-T100LC AccuTOF mass spectrometer (ESI-TOF, positive mode; JEOL Ltd.). Optical rotations were recorded with a Jasco DIP-1000 digital polarimeter. Circular dichroism spectra were recorded with a Jasco J-820 spectrophotometer. Column chromatography was performed using silica gel (Wakogel C-200, Wako Pure Chemical Industries, Ltd., Osaka, Japan).

Synthesis of PAO*n* (*n*=1-6) (15-20)

6-((*tert*-butyldimethylsilyl)oxy)-2,2-dimethyl-3,4-dihydronaphthalen-1(2H)-one (8)

To a suspension of NaH (13.6 g, 341 mmol) in dry THF (100 mL) was added 6-methoxy-1-tetralone **5** (10.0 g, 56.8 mmol) dissolved in THF (35 mL). After stirring the mixture for 15 min at room temperature, methyl iodide (9.2 mL, 150 mmol) was added dropwise to the mixture. The mixture was stirred for 2 h at room temperature. After quenching with water (100 mL), it was then extracted with EtOAc (200 mL × 3), washed with brine, dried over Na_2SO_4. Evaporation of solvent *in vacuo* yielded the crude dimethyl tetralone **6**, as brown oil (13.4 g). To the dimethyl tetralone **6** (13.4 g) was added an excess amount of 48% hydrobromic acid (250 mL) and the mixture refluxed for 4.5 h. After quenching with ice/water, it was the extracted with EtOAc (350 mL × 3). The organic phase was the re-extracted with 1M NaOH and allowed to stand for an hour. The aqueous phase was then acidified with 2 M HCl and extracted with EtOAc (300 mL × 3). The organic phase was washed with brine and died over Na_2SO_4. Evaporation of solvent *in vacuo* yielded the crude product **7** (8.5 g) as a brown solid. To a suspension of 6-hydroxy-2,2-dimethyl-1-tetralone **7** (8.5 g, 45 mmol) and imidazole (7.6 g, 110 mmol) in anhydrous DMF (90 mL), was added *t*-buthyldimethylsilylchloride (10.8 g, 71.5 mmol). The reaction mixture was stirred for 90 min at room temperature. After quenching with sat. NH_4Cl (90 mL), it was extracted with EtOAc (100 mL × 3). The organic layer was washed with brine, dried over Na_2SO_4, and concentrated *in vacuo*. The residual oil was purified by silica gel column chromatography with 3% EtOAc in hexane to obtain **8** (7.2 g, 53% from **5**) as a yellow solution. ^{1}H NMR (270 MHz, $CDCl_3$): δ_H 0.23 (6H, s, 2 × CH_3-Si), 0.99 (9H, s, *t*-butyl), 1.20 (6H, s, H_3-8′ and 9′), 1.95 (2H, t, *J*=6.3 Hz, H_2-5′), 2.90 (2H, t, *J*=6.3 Hz, H_2-4′), 6.62 (1H, d, *J*=2.6 Hz, H-12′), 6.74 (1H, dd, *J*=8.6 and 2.6 Hz, H-10′), 7.96 (1H, d, *J*=8.6 Hz, H-7′); ^{13}C NMR (68 MHz,

$CDCl_3$): δ_C −4.4, −4.4, 18.2, 24.5, 24.5, 25.6, 25.6, 25.6, 25.9, 36.7, 41.3, 118.8, 118.9, 125.5, 130.3, 145.7, 160.0, 201.9. HRMS (*m/z*): $[M+H]^+$ calcd. for $C_{18}H_{29}O_2Si$, 305.1937; found, 305.1934.

(*Z*)-6-((*tert*-butyldimethylsilyl)oxy)-1-(5-hydroxy-3-methylpent-3-en-1-yn-1-yl)-2,2-dimethyl-1,2,3,4-tetrahydronaphthalen-1-ol (9)

(*Z*)-3-Mehylpent-2-en-4-yn-1-ol (side chain) (4.04 g, 42.0 mmol) in dry THF (120 mL) was cooled to −80 °C under an atmosphere of Ar. *n*-Butyllithium (51.0 mL, 1.65 M) was then added slowly. After being stirred for 45 min at −80 °C, a solution of the silyl protected tetralone **8** (8.00 g, 26.3 mmol) in dry THF (10 mL) was added dropwise to the stirred mixture. The reaction mixture was stirred for a further 20 min at −80 °C and then the ice bath was removed. The reaction mixture was stirred at room temperature for 60 min. After quenching with sat. NH_4Cl (100 mL), it was extracted with EtOAc (200 mL × 3). The organic layer was washed with brine, dried over Na_2SO_4, and concentrated *in vacuo*. The residual oil was purified by silica gel chromatography with 20% EtOAc in hexane to obtain **9** (5.60 g, 54%) as a yellow oil. ^{1}H NMR (270 MHz, CD_3OD): δ_H 0.14 (6H, s, 2 × CH_3-Si), 0.94 (9H, s, *t*-butyl), 1.02 (3H, s, H_3-8′ or 9′), 1.09 (3H, s, H_3-8′ or 9′), 1.59 (1H, dt, *J*=13.3 and 6.0 Hz, H-5′), 1.87 (3H, q, *J*=1.3 Hz, H_3-6), 1.93 (1H, dt, *J*=13.3 and 8.6 Hz, H-5′), 2.73 (2H, dd, *J*=8.6 and 6.0 Hz, H_2-4′), 4.22 (2H, dq, *J*=6.6 and 1.3 Hz, H_2-1), 5.77 (1H, tq, *J*=6.6 and 1.3 Hz, H-2), 6.51 (1H, d, *J*=2.6 Hz, H-12′), 6.64 (1H, dd, *J*=8.6 and 2.6 Hz, H-10′), 7.61 (1H, d, *J*=8.6 Hz, H-7′); ^{13}C NMR (68 MHz, CD_3OD): δ_C −4.3, −4.3, 19.1, 23.3, 24.3, 24.5, 26.1, 26.1, 26.1, 26.9, 32.4, 38.7, 61.7, 75.5, 85.0, 98.1, 119.1, 120.5, 121.0, 131.2, 133.9, 136.9, 137.7, 156.3. HRMS (*m/z*): $[M+Na]^+$ calcd. for $C_{24}H_{36}O_3SiNa$, 423.2331; found, 423.2338.

6-((*tert*-butyldimethylsilyl)oxy)-1-((1*E*,3*Z*)-5-hydroxy-3-methylpenta-1,3-dien-1-yl)-2,2-dimethyl-1,2,3,4-tetrahydronaphthalen-1-ol (10)

To a stirred solution of **9** (4.38 g, 10.9 mmol) in dry THF (95 mL) was cooled to −18 °C and added sodium bis (2-methoxyethoxy) aluminum hydride in toluene 65 % w/w (SMEAH) (10.8 mL, 36.0 mmol) under an atmosphere of Ar. The mixture was stirred for 60 min at room temperature. After quenching with sat. NH_4Cl (45 mL), it was diluted with water (40 mL) and extracted with EtOAc (80 mL × 3). The organic layer was washed with brine, dried over Na_2SO_4, and concentrated *in vacuo*. The residual oil was purified by silica gel chromatography with hexane-EtOAc stepwise to obtain **10** (3.05 g, 69%) as a yellow oil. ^{1}H NMR (270 MHz, CD_3OD): δ_H 0.14 (6H, s, 2 × CH_3-Si), 0.93 (3H, s, H_3-8′ or 9′), 0.94 (3H, s, H_3-8′ or 9′), 0.95 (9H, s, *t*-butyl), 1.59 (1H, dt, *J*=13.5 and 6.6 Hz, H-5′), 1.77 (1H, dt, *J*=13.5 and 6.6 Hz, H-5′), 1.80 (3H, d, *J*=1.0, H_3-6), 2.74 (2H, m, H_2-4′), 4.12 (2H, d, *J*=6.6 Hz, H_2-1), 5.43 (1H, tq, *J*=6.6 and 1.0 Hz, H-2), 5.93 (1H, d, *J*=15.5 Hz, H-4), 6.44, (1H, d, *J*=15.5 Hz, H-5) 6.52 (1H, d, *J*=2.6 Hz, H-12′), 6.59 (1H, dd, *J*=8.6 and 2.6 Hz, H-10′), 7.17 (1H, d, *J*=8.6 Hz, H-7′); ^{13}C NMR (68 MHz, CD_3OD): δ_C −4.3, −4.3, 19.1, 20.9, 23.7, 24.6,

26.2, 26.2, 26.2, 27.1, 34.2, 38.2, 58.6, 79.1, 119.1, 120.3, 127.1, 129.4, 131.1, 134.9, 135.2, 137.2, 138.6, 155.8. HRMS (*m/z*): $[M+Na]^+$ calcd. for $C_{24}H_{38}O_3SiNa$, 425.2488; found, 425.2486.

(2*Z*,4*E*)-methyl 5-(6-((*tert*-butyldimethylsilyl)oxy)-1-hydroxy-2,2-dimethyl-1,2,3,4-tetrahydronaphthalen-1-yl)-3-methylpenta-2,4-dienoate (12)

To a stirred solution of **10** (3.05g, 7.57 mmol) in dry acetone (100 mL) was added MnO_2 (13.2 g, 129 mmol) at room temperature. After string at room temperature for 30 min, all the starting material had disappeared. The reaction mixture was then filtered through a pad of Celite® and concentrated *in vacuo*. The crude material (2.99 g) was carried through to the next stage without further purification. The crude tetralone aldehyde **11** (2.99 g, 7.46 mmol) was dissolved in methanol (50 mL) and stirred with MnO_2 (13.2 g, 129 mmol), NaCN (1.11 g, 22.7 mmol) and AcOH (0.43 mL, 7.6 mmol) at room temperature. After 60 min, the reaction mixture was filtered through a pad of Celite® and concentrated *in vacuo*. The residue was brought up in distilled H_2O and extracted with EtOAc (80 mL × 3). The organic layer was washed with brine, dried over Na_2SO_4, and concentrated *in vacuo*. The residual oil was purified by silica gel chromatography with 7.5% EtOAc in hexane to obtain **12** (1.54 g, 47%) as a yellow oil. ^{1}H NMR (270 MHz, $CDCl_3$): δ_H 0.19 (6H, s, 2 × CH_3-Si), 0.96 (3H, s, H_3-8′ or 9′), 0.97 (9H, s, *t*-butyl), 1.01 (3H, s, H_3-8′ or 9′), 1.64 (1H, dt, *J*=13.8 and 6.9 Hz, H-5′), 1.75 (1H, s, -OH), 1.91 (1H, dt, *J*=13.8 and 6.9 Hz, H-5′), 2.01 (3H, d, *J*=1.0, H_3-6), 2.80 (2H, t, *J*=6.9 Hz, H_2-4′), 3.70 (3H, s, -OCH_3), 5.69 (1H, s, H-2), 6.32 (1H, d, *J*=16.1 Hz, H-5), 6.57 (1H, d, *J*=2.3 Hz, H-12′), 6.63 (1H, dd, *J*=8.2 and 2.3 Hz, H-10′), 7.20 (1H, d, *J*=8.2 Hz, H-7′), 7.82 (1H, d, *J*=16.1 Hz, H-4); ^{13}C NMR (68 MHz, $CDCl_3$): δ_C −4.4, −4.4, 18.1, 21.3, 23.2, 24.0, 25.7, 25.7, 25.7, 26.1, 33.0, 37.2, 51.0, 77.7, 116.8, 118.3, 119.6, 126.5, 129.5, 133.2, 137.1, 141.6, 150.5, 154.7, 166.6. HRMS (*m/z*): $[M+Na]^+$ calcd. for $C_{25}H_{38}O_4SiNa$, 453.2437; found, 453.2433.

(2*Z*,4*E*)-methyl 5-(6-((*tert*-butyldimethylsilyl)oxy)-1-hydroxy-2,2-dimethyl-4-oxo-1,2,3,4-tetrahydronaphthalen-1-yl)-3-methylpenta-2,4-dienoate (13)

The methyl ester **12** (1.52 g, 3.54 mmol) in dry benzene (15 mL) was added Celite® (7 g) and pyridinium dichromate (5.33 g, 14.2 mmol). After being stirred for 20 min, 70% *tert*-butyl hydroperoxide (2.66 mL, 18.6 mmol) was added to the mixture. The reaction mixture was stirred for 2 h at room temperature, and then diluted with diethyl ether (25 mL) and filtered over a bed of Celite®. Evaporation of solvent *in vacuo* and residual oil was purified by silica gel column chromatography with hexane-EtOAc stepwise to obtain **13** (0.43 g, 27%) as a yellow oil. ^{1}H NMR (270 MHz, $CDCl_3$): δ_H 0.22 (6H, s, 2 × CH_3-Si), 0.98 (9H, s, *t*-butyl), 1.07 (6H, s, H_3-8′ and 9′), 2.02 (3H, d *J*=1.3 Hz, H_3-6), 2.07 (1H, s, -OH), 2.55 (1H, d, *J*=16.8 Hz, H-5′), 2.85 (1H, d, *J*=16.8 Hz,

H-5′), 3.70 (3H, s, -O*CH*$_3$), 5.74 (1H, s, H-2), 6.37 (1H, d, *J*=16.1 Hz, H-5), 7.04 (1H, dd, *J*=8.6 and 2.6 Hz, H-10′), 7.38 (1H, d, *J*=8.6 Hz, H-7′), 7.46 (1H, d, *J*=2.6 Hz, H-12′), 7.87 (1H, d, *J*=16.1 Hz, H-4); ^{13}C NMR (125 MHz, $CDCl_3$): δ_C −4.5, −4.5, 18.2, 21.2, 23.5, 24.4, 25.6, 25.6, 25.6, 41.1, 49.8, 51.1, 77.9, 117.0, 117.9, 126.4, 128.0,128.8, 132.3, 138.5, 138.7, 149.6, 155.7, 166.4, 197.1. HRMS (*m/z*): $[M+Na]^+$ calcd. for $C_{25}H_{36}O_5SiNa$, 467.2230; found, 467.2236.

(2*Z*,4*E*)-methyl 5-(1,6-dihydroxy-2,2-dimethyl-4-oxo-1,2,3,4-tetrahydronaphthalen-1-yl)-3-methylpenta-2,4-dienoate (14)

To the silyl protected ester **13** (0.48 g, 1.1 mmol) in tetraethylene glycol (11 mL) was added potassium fluoride (94 mg, 1.6 mmol). The reaction mixture was stirred for 60 min at room temperature. After quenching with water (50 mL), it was extracted with EtOAc (40 mL × 3). The organic layer was washed with brine, dried over Na_2SO_4, and concentrated *in vacuo*. The residual oil was purified by silica gel chromatography with 35% EtOAc in hexane to obtain **14** (0.36 g, quantitative yield) as a pale yellow oil. ^{1}H NMR (270 MHz, $CDCl_3$): δ_H 1.06 (3H, s, H_3-8′ or 9′), 1.07 (3H, s, H_3-8′ or 9′), 2.02 (3H, d *J*=1.3 Hz, H_3-6), 2.45 (1H, br s, -OH), 2.53 (1H, d, *J*=16.8 Hz, H-5′), 2.91 (1H, d, *J*=16.8 Hz, H-5′), 3.71 (3H, s, -O*CH*$_3$), 5.76 (1H, s, H-2), 6.23 (1H, br s, -OH), 6.38 (1H, d, *J*=16.1 Hz, H-5), 6.97 (1H, dd, *J*=8.6 and 3.0 Hz, H-10′), 7.32 (1H, d, *J*=8.6 Hz, H-7′), 7.48 (1H, d, *J*=3.0 Hz, H-12′), 7.85 (1H, d, *J*=16.1 Hz, H-4); ^{13}C NMR (68 MHz, $CDCl_3$): δ_C 21.3, 23.6, 24.4, 41.2, 49.7, 51.3, 77.8, 112.4, 117.8, 121.9, 128.2, 129.3, 132.1, 138.0, 138.7, 150.0, 155.8, 166.8, 197.7; HRMS (*m/z*): $[M+Na]^+$ calcd. for $C_{19}H_{22}O_5Na$, 353.1365; found, 353.1359.

(2*Z*,4*E*)-5-(1-hydroxy-6-methoxy-2,2-dimethyl-4-oxo-1,2,3,4-tetrahydronaphthalen-1-yl)-3-methylpenta-2,4-dienoic acid, (±)-PAO1 (15)

To a suspension of **14** (36.6 mg, 0.11 mmol) and K_2CO_3 (31 mg, 0.22 mmol) in anhydrous DMF (0.8 mL), was added methyl iodide (14 μL, 0.22 mmol). The reaction mixture was heated to 70 °C and stirred for 80 min. After quenching with water H_2O (10 mL), it was extracted with EtOAc (15 mL × 3). The organic layer was washed with brine, dried over Na_2SO_4, and concentrated *in vacuo*. The residual oil was purified by silica gel chromatography with 25% EtOAc in hexane to obtain PAO1-methyl ester (34.7 mg) as pale yellow oil. A solution of 1 M NaOH (10 mL) was added to a solution of PAO1-methyl ester (34.7 mg) in MeOH (10 mL), and reaction mixture was stirred for 60 min at room temperature. The pH of the reaction mixture was adjusted to 2 using 2 M HCl, it was diluted with H_2O (10 mL) and extracted with EtOAc (15 mL × 3). The organic layer was washed with brine, dried over Na_2SO_4, and concentrated *in vacuo*. The residual oil was purified by silica gel chromatography with 45% EtOAc in hexane containing 0.1% AcOH to obtain **(±)-PAO1** (30.5 mg, 84%) as pale yellow oil. ^{1}H NMR (500 MHz, acetone-d_6): δ_H 1.05 (3H, s, H_3-8′ or 9′), 1.09 (3H, s,

H_3-8′ or 9′), 2.04 (3H, br s, H_3-6), 2.63 (1H, d, *J*=16.6 Hz, H-5′), 2.73 (1H, d, *J*=16.6 Hz, H-5′), 3.85 (3H, s, H_3-1″), 5.74 (1H, s, H-2), 6.55 (1H, d, *J*=15.9 Hz, H-5), 7.16 (1H, dd, *J*=8.5 and 2.7 Hz, H-10′), 7.41 (1H, d, *J*=2.7 Hz, H-12′), 7.53 (1H, d, *J*=8.5 Hz, H-7′), 7.90 (1H, d, *J*=15.9 Hz, H-4); ^{13}C NMR (125 MHz, acetone-d_6): δ_C 21.2 (C6), 23.9 (C8′ or 9′), 24.6 (C8′ or 9′), 41.8 (C6′), 50.4 (C5′), 55.7 (C1″), 78.1 (C1′), 109.4 (C12′), 119.0 (C-2), 121.6 (C-10′), 128.5 (C4), 130.5 (C7′), 133.1 (C2′), 139.9 (C3′), 140.5 (C5), 150.4 (C3), 160.0 (C11′), 167.8 (C1), 197.1 (C4′); UV λ_{max} (MeOH) nm (ε): 221.2 (23,800), 255.6 (21,900), 319.4 (3,000); HRMS (*m/z*): $[M+Na]^+$ calcd. for $C_{19}H_{22}O_5Na$, 353.1365; found, 353.1358.

A Chiralcel OD HPLC column (250 × 10.0 mm i.d., Daicel; solvent, 6% 2-propanal in hexane containing 0.05% TFA; flow rate, 4.7 ml/min; detection, 254 nm) was injected with (±)-PAO1. The material at t_R 18.7 and 24.1 min were collected to give (−)-PAO1 (4.7 mg) and the (+)-enantiomer (4.6 mg) with an optical purity of 99.4% and 98.5%, respectively. (+)-PAO1: $[\alpha]_D^{26}$ +229.1 (MeOH; *c* 0.194); CD λ_{ext} (MeOH) nm (Δε): 258.0 (13.3), 225.0 (−16.8). (−)-PAO1: $[\alpha]_D^{26}$ −208.2 (MeOH; *c* 0.187); CD λ_{ext} (MeOH) nm (Δε): 257.0 (−12.6), 223.0 (14.0).

(2*Z*,4*E*)-5-(6-ethoxy-1-hydroxy-2,2-dimethyl-4-oxo-1,2,3,4-tetrahydronaphthalen-1-yl)-3-methylpenta-2,4-dienoic acid, (±)-PAO2 (16)

To a suspension of **14** (18.2 mg, 0.06 mmol) and K_2CO_3 (15 mg, 0.11 mmol) in anhydrous DMF (0.8 mL), was added ethyliodide (12 μL, 0.14 mmol). The reaction mixture was heated to 70 °C and stirred for 2.5 h. After quenching with water H_2O (10 mL), it was extracted with EtOAc (10 mL × 3). The organic layer was washed with brine, dried over Na_2SO_4, and concentrated *in vacuo*. The residual oil was purified by silica gel chromatography with 30% EtOAc in hexane to obtain PAO2-methyl ester (16.1 mg) as pale yellow oil. A solution of 2 M NaOH (5 mL) was added to a solution of PAO2-methyl ester (16.1 mg) in MeOH (10 mL), and reaction mixture was stirred for 2 h at room temperature. The pH of the reaction mixture was adjusted to 2 using 2 M HCl, it was diluted with H_2O (10 mL) and extracted with EtOAc (20 mL × 3). The organic layer was washed with brine, dried over Na_2SO_4, and concentrated *in vacuo*. The residual oil was purified by silica gel chromatography with 40% EtOAc in hexane containing 0.1% AcOH to obtain **(±)-PAO2** (15.0 mg, 79%) as pale yellow oil. ^{1}H NMR (500 MHz, acetone-d_6): δ_H 1.04 (3H, s, H_3-8′ or 9′), 1.07 (3H, s, H_3-8′ or 9′), 1.37 (3H, t, *J*=7.0 Hz, H_3-2″), 2.02 (3H, br s, H_3-6), 2.63 (1H, d, *J*=16.6 Hz, H-5′), 2.73 (1H, d, *J*=16.6 Hz, H-5′), 4.08 (2H, q, *J*=7.0 Hz, H_2-1″), 5.72 (1H, s, H-2), 6.52 (1H, d, *J*=15.9 Hz, H-5), 7.13 (1H, dd, *J*=8.5 and 2.7 Hz, H-10′), 7.37 (1H, d, *J*=2.7 Hz, H-12′), 7.50 (1H, d, *J*=8.5 Hz, H-7′), 7.89(1H, d, *J*=15.9 Hz, H-4); ^{13}C NMR (125 MHz, acetone-d_6): δ_C 15.0 (C2″), 21.2 (C6), 23.9 (C8′ or 9′), 24.6 (C8′ or 9′), 41.8 (C6′), 50.4 (C5′), 64.3 (C1″), 78.1 (C1′), 110.1 (C12′), 119.2 (C-2), 122.0 (C-10′), 128.5 (C4), 130.5 (C7′), 133.1 (C2′), 139.8 (C3′), 140.4 (C5), 150.3 (C3), 159.3 (C11′), 167.9 (C1), 197.2 (C4′); UV λ_{max} (MeOH) nm (ε): 222.4 (24,300), 256.2 (23,100), 319.8

(3,100); HRMS (*m/z*): $[M+Na]^+$ calcd. for $C_{20}H_{24}O_5Na$, 367.1521; found, 367.1508.

(2*Z*,4*E*)-5-(1-hydroxy-2,2-dimethyl-4-oxo-6-propoxy-1,2,3,4-tetrahydronaphthalen-1-yl)-3-methylpenta-2,4-dienoic acid, (±)-PAO3 (17)

To a suspension of **14** (36.6 mg, 0.11 mmol) and K_2CO_3 (31 mg, 0.22 mmol) in anhydrous DMF (0.8 mL), was added 1-iodopropane (27 μL, 0.22 mmol). The reaction mixture was heated to 70 °C and stirred for 100 min. After quenching with water H_2O (10 mL), it was extracted with EtOAc (20 mL × 3). The organic layer was washed with brine, dried over Na_2SO_4, and concentrated *in vacuo*. The residual oil was purified by silica gel chromatography with 20% EtOAc in hexane to obtain PAO3-methyl ester (38.7 mg) as pale yellow oil. A solution of 2 M NaOH (10 mL) was added to a solution of PAO3-methyl ester (31.5 mg) in MeOH (10 mL), and reaction mixture was stirred for 60 min at room temperature. The pH of the reaction mixture was adjusted to 2 using 2 M HCl, it was diluted with H_2O (10 mL) and extracted with EtOAc (20 mL × 3). The organic layer was washed with brine, dried over Na_2SO_4, and concentrated *in vacuo*. The residual oil was purified by silica gel chromatography with 40% EtOAc in hexane containing 0.1% AcOH to obtain **(±)-PAO3** (28.5 mg, 85%) as pale yellow oil. ^{1}H NMR (500 MHz, CD_3OD): δ_H 1.03 (3H, s, H_3-8′ or 9′), 1.04 (3H, d, J=6.7 Hz, H_3-3″), 1.07 (3H, s, H_3-8′ or 9′), 1.80 (2H, tq, *J*=6.7 and 6.7 Hz, H_2-2″), 2.02 (3H, br s, H_3-6), 2.59 (1H, d, *J*=16.0 Hz, H-5′), 2.72 (1H, d, *J*=16.0 Hz, H-5′), 3.98 (2H, t, *J*=6.7 Hz, H_2-1″), 5.72 (1H, s, H-2), 6.44 (1H, d, *J*=15.8 Hz, H-5), 7.18 (1H, dd, *J*=8.5 and 2.7 Hz, H-10′), 7.42 (1H, d, *J*=2.7 Hz, H-12′), 7.48 (1H, d, *J*=8.5 Hz, H-7′), 7.64 (1H, d, *J*=15.8 Hz, H-4); ^{13}C NMR (125 MHz, CD_3OD): δ_C 10.8 (C3″), 21.3 (C6), 23.6 (C2″), 24.0 (C8′ or 9′), 24.7 (C8′ or 9′), 42.4 (C6′), 50.9 (C5′), 70.8 (C1″), 78.8 (C1′), 110.6 (C12′), 120.1 (C-2), 122.9 (C-10′), 129.6 (C4), 130.8 (C7′), 133.4 (C2′), 140.2 (C3′), 140.5 (C5), 150.2 (C3), 160.1 (C11′), 170.1 (C1), 199.8 (C4′); UV λ_{max} (MeOH) nm (ε): 222.8 (26,900), 255.6 (23,600), 321.2 (3,200); HRMS (*m/z*): $[M+Na]^+$ calcd. for $C_{21}H_{26}O_5Na$, 381.1673; found, 381.1678.

(2*Z*,4*E*)-5-(6-butoxy-1-hydroxy-2,2-dimethyl-4-oxo-1,2,3,4-tetrahydronaphthalen-1-yl)-3-methylpenta-2,4-dienoic acid, (±)-PAO4 (18)

To a suspension of **14** (20.5 mg, 0.06 mmol) and K_2CO_3 (17 mg, 0.12 mmol) in anhydrous DMF (0.8 mL), was added 1-iodobutane (18 μL, 0.16 mmol). The reaction mixture was heated to 70 °C and stirred for 120 min. After quenching with water H_2O (10 mL), it was extracted with EtOAc (10 mL × 3). The organic layer was washed with brine, dried over Na_2SO_4, and concentrated *in vacuo*. The residual oil was purified by silica gel chromatography with 20% EtOAc in hexane to obtain PAO4-methyl ester (20.7 mg) as pale yellow oil. A solution of 2 M NaOH (6 mL) was added to a solution of PAO4-methyl ester (20.7 mg) in MeOH (10 mL), and reaction mixture was stirred for 3 h at room temperature. The pH of the reaction mixture was adjusted to 2 using 2 M HCl, it was diluted

with H_2O (10 mL) and extracted with EtOAc (20 mL × 3). The organic layer was washed with brine, dried over Na_2SO_4, and concentrated *in vacuo*. The residual oil was purified by silica gel chromatography with 35% EtOAc in hexane containing 0.1% AcOH to obtain **(±)-PAO4** (16.9 mg, 73%) as pale yellow oil. ^{1}H NMR (500 MHz, CD_3OD): δ_H 0.98 (3H, t, *J*=7.3 Hz, H_3-4″), 1.02 (3H, s, H_3-8′ or 9′), 1.06 (3H, s, H_3-8′ or 9′), 1.51 (2H, tq, *J*=7.3 and 7.3 Hz, H_2-3″), 1.76 (2H, m, H_2-2″), 2.01 (3H, s, H_3-6), 2.58 (1H, d, *J*=16.5 Hz, H-5′), 2.71 (1H, d, *J*=16.5 Hz, H-5′), 4.02 (2H, t, *J*=6.4 Hz, H_2-1″), 5.72 (1H, s, H-2), 6.43 (1H, d, *J*=15.9 Hz, H-5), 7.17 (1H, dd, *J*=8.8 and 2.7 Hz, H-10′), 7.41 (1H, d, *J*=2.7 Hz, H-12′), 7.47 (1H, d, *J*=8.8 Hz, H-7′), 7.62 (1H, d, *J*=15.9 Hz, H-4); ^{13}C NMR (125 MHz, CD_3OD): δ_C 14.2 (C4″), 20.3 (C3″), 21.3 (C6), 24.0 (C8′ or 9′), 24.7 (C8′ or 9′), 32.4 (C2″), 42.4 (C6′), 50.9 (C5′), 69.0 (C1″), 78.8 (C1′), 110.5 (C12′), 119.4 (C-2), 122.9 (C-10′), 129.5 (C4), 130.8 (C7′), 133.4 (C2′), 140.2 (C3′), 140.7 (C5), 1501.1 (C3), 160.1 (C11′), 169.6 (C1), 199.8 (C4′). (C1); UV λ_{max} (MeOH) nm (ε): 222.6 (26,600), 256.0 (23,000), 322.0 (3,100); HRMS (*m/z*): $[M+Na]^+$ calcd. for $C_{22}H_{28}O_5Na$, 395.1834; found, 395.1838.

A Chiralcel OD HPLC column (250 × 10.0 mm i.d., Daicel; solvent, 6% 2-propanal in hexane containing 0.05% TFA; flow rate, 4.0 ml/min; detection, 254 nm) was injected with (±)-PAO4. The material at t_R 16.0 and 25.9 min were collected to give (−)-PAO4 (10.1 mg) and the (+)-enantiomer (10.1 mg) with an optical purity of 97.1% and 98.9%, respectively. (+)-PAO4: $[\alpha]_D^{25}$ +214.6 (MeOH; *c* 0.50); CD λ_{ext} (MeOH) nm (Δε): 261.0 (14.7), 224.0 (−19.3). (−)-PAO1: $[\alpha]_D^{25}$ −211.8 (MeOH; *c* 0.50); CD λ_{ext} (MeOH) nm (Δε): 261.0 (−14.6), 224.0 (17.0).

(2*Z*,4*E*)-5-(1-hydroxy-2,2-dimethyl-4-oxo-6-(pentyloxy)-1,2,3,4-tetrahydronaphthalen-1-yl)-3-methylpenta-2,4-dienoic acid, (±)-PAO5 (19)

To a suspension of **14** (33.2 mg, 0.10 mmol) and K_2CO_3 (28 mg, 0.20 mmol) in anhydrous DMF (0.8 mL), was added 1-iodopentane (33 μL, 0.25 mmol). The reaction mixture was heated to 70 °C and stirred for 2 h. After quenching with water H_2O (10 mL), it was extracted with EtOAc (20 mL × 3). The organic layer was washed with brine, dried over Na_2SO_4, and concentrated *in vacuo*. The residual oil was purified by silica gel chromatography with 20% EtOAc in hexane to obtain PAO5-methyl ester (37.1 mg) as pale yellow oil. A solution of 2 M NaOH (6 mL) was added to a solution of PAO5-methyl ester (32.5 mg) in MeOH (10 mL), and reaction mixture was stirred for 2 h at room temperature. The pH of the reaction mixture was adjusted to 2 using 2 M HCl, it was diluted with H_2O (10 mL) and extracted with EtOAc (20 mL × 3). The organic layer was washed with brine, dried over Na_2SO_4, and concentrated *in vacuo*. The residual oil was purified by silica gel chromatography with 30% EtOAc in hexane containing 0.1% AcOH to obtain **(±)-PAO5** (29.3 mg, 86%) as pale yellow oil. ^{1}H NMR (500 MHz, CD_3OD): δ_H 0.93 (3H, t, *J*=7.3 Hz, H_3-5″), 1.02 (3H, s, H_3-8′ or 9′), 1.06 (3H, s, H_3-8′ or 9′), 1.39 (2H, m, H_2-4″), 1.44 (2H, m, H_2-3″), 1.77 (2H, m, H_2-2″), 2.01 (3H, s, H_3-6), 2.58 (1H, d, *J*=16.2 Hz, H-5′), 2.70 (1H, d, *J*=16.2 Hz, H-5′), 4.00 (2H, t, *J*=6.4

Hz, H_2-1″), 5.71 (1H, s, H-2), 6.45 (1H, d, *J*=15.9 Hz, H-5), 7.16 (1H, dd, *J*=8.9 and 2.7 Hz, H-10′), 7.40 (1H, d, *J*=2.7 Hz, H-12′), 7.47 (1H, d, *J*=8.9 Hz, H-7′), 7.64 (1H, d, *J*=15.9 Hz, H-4); ^{13}C NMR (125 MHz, CD_3OD): δ_C 14.4 (C5″), 21.3 (C6), 23.5 (C4″), 24.0 (C8′ or 9′), 24.7 (C8′ or 9′), 29.3 (C3″), 30.0 (C2″), 42.4 (C6′), 50.9 (C5′), 69.3 (C1″), 78.8 (C1′), 110.5 (C12′), 119.7 (C-2), 122.9 (C-10′), 129.5 (C4), 130.8 (C7′), 133.3 (C2′), 140.2 (C3′), 140.5 (C5), 150.6 (C3), 160.1 (C11′), 169.9 (C1), 199.8 (C4′); UV λ_{max} (MeOH) nm (ε): 223.2 (27,900), 255.8 (24,000), 320.4 (3,200); HRMS (*m/z*): $[M+Na]^+$ calcd. for $C_{23}H_{30}O_5Na$, 409.1989; found, 409.1991.

(2*Z*,4*E*)-5-(6-(hexyloxy)-1-hydroxy-2,2-dimethyl-4-oxo-1,2,3,4-tetrahydronaphthalen-1-yl)-3-methylpenta-2,4-dienoic acid, (±)-PAO6 (20)

To a suspension of **14** (70.2 mg, 0.21 mmol) and K_2CO_3 (44 mg, 0.32 mmol) in anhydrous DMF (1.3 mL), was added 1-iodohexane (50 μL, 0.32 mmol). The reaction mixture was heated to 60 °C and stirred for 2 h. After quenching with water H_2O (10 mL), it was extracted with EtOAc (20 mL × 3). The organic layer was washed with brine, dried over Na_2SO_4, and concentrated *in vacuo*. The residual oil was purified by silica gel chromatography with 15% EtOAc in hexane to obtain PAO6-methyl ester (78.8 mg) as pale yellow oil. A solution of 2 M NaOH (30 mL) was added to a solution of PAO6-methyl ester (77.7 mg) in MeOH (35 mL), and reaction mixture was stirred for 3 h at room temperature. The pH of the reaction mixture was adjusted to 2 using 2 M HCl, it was extracted with EtOAc (50 mL × 3). The organic layer was washed with brine, dried over Na_2SO_4, and concentrated *in vacuo*. The residual oil was purified by silica gel chromatography with EtOAc-hexane stepwise containing 0.1% AcOH to obtain **(±)-PAO6** (68.8 mg, 81%) as pale yellow oil. ^{1}H NMR (500 MHz, CD_3OD): δ_H 0.87 (3H, t, *J*=7.0 Hz, H_3-6″), 0.98 (3H, s, H_3-8′ or 9′), 1.02 (3H, s, H_3-8′ or 9′), 1.31 (4H, m, H_2-4″ and 5″), 1.44 (2H, m, H_2-3″), 1.73 (2H, m, H_2-2″), 1.97 (3H, d, *J*=0.9 Hz, H_3-6), 2.54 (1H, d, *J*=16.2 Hz, H-5′), 2.67 (1H, d, *J*=16.2 Hz, H-5′), 3.96 (2H, t, *J*=6.4 Hz, H_2-1″), 5.67 (1H, s, H-2), 6.40 (1H, d, *J*=15.8 Hz, H-5), 7.12 (1H, dd, *J*=8.5 and 2.7 Hz, H-10′), 7.37 (1H, d, *J*=2.7 Hz, H-12′), 7.43 (1H, d, *J*=8.5 Hz, H-7′), 7.60 (1H, d, *J*=15.8 Hz, H-4); ^{13}C NMR (125 MHz, CD_3OD): δ_C 14.4 (C6″), 21.3 (C6), 23.6 (C5″), 24.0 (C8′ or 9′), 24.7 (C8′ or 9′), 26.8 (C3″), 30.3 (C2″), 32.7 (C4″), 42.4 (C6′), 50.9 (C5′), 69.3 (C1″), 78.8 (C1′), 110.5 (C12′), 119.9 (C-2), 122.9 (C-10′), 129.6 (C4), 130.8 (C7′), 133.4 (C2′), 140.2 (C3′), 140.4 (C5), 150.3 (C3), 160.1 (C11′), 170.0 (C1), 199.8 (C4′); UV λ_{max} (MeOH) nm (ε): 222.8 (28,000), 255.4 (23,800), 320.4 (3,100); HRMS (*m/z*): $[M+Na]^+$ calcd. for $C_{24}H_{32}O_5Na$, 423.2149; found, 423.2147.

***Arabidopsis* seed germination assay**

Twenty to thirty-five seeds (Columbia accession) were sterilized successively with soaking in 70% aqueous ethanol (EtOH, v/v) for 30 min and reagent-grade EtOH for 1 min. They were then soaked

in distilled water and incubated in darkness at 5 °C for 3 d. The stratified seeds then soaked in 100 μL of a test medium liquid agar in 96-well plates and allowed to germinate under continuous illumination at 22 °C. All of the assays were conducted at least three times.

Lettuce seed germination assay

Twenty-five seeds (*Lactuca sativa* L. cv. Cisco) were placed in a dish on two sheets of filter paper soaked in 2 mL of a test solution and allowed to germinate and grow at 22 °C and under continuous illumination.

PP2C enzyme assay

The protocol of PP2C enzyme assay has been described elsewhere[14]. Briefly, the proteins of PYLs and HAB1 were expressed in *E. coli* and purified by affinity column chromatography. Purified proteins were preincubated in 80 μL of buffer containing 12.5 mM $MnCl_2$, 0.125% 2-mercaptoethanol and test compound at 22 °C for 30 min. After adding 20 μL of substrate buffer (165 mM Tris-acetate, pH 7.9, 330 mM potassium acetate, 0.1% BSA and 250 mM *p*NPP), reactions were immediately monitored for hydrolysis of *p*NPP at 405 nm. The PP2C assay was performed using 60 pmol each of PP2C and PYL.

Isothermal titration calorimetry

(+)-PAO*n*-binding studies were performed by isothermal titration calorimetry (ITC) using an iTC_{200} calorimeter (Microcal, GE Healthcare Bio-Sciences AB) and were conducted at 20 °C and with a solvent of 100 mM phosphate buffer, pH 8.0. His_6-tagged PYL5 or His_6-tagged PYL10 were assayed at a concentration of 34 μM and 50 μM, respectively, with (+)-PAO1 and (+)-PAO4 stock solutions in the injection syringe at tenfold higher concentrations than the proteins. All of the titrations were carried out via a series of 25 injections of 1.25 μL each. The data were corrected by subtracting the mixing enthalpies for the (+)-PAO4 or (+)-PAO1 solutions into protein-free solutions and fitted by Origin for ITC (GE Healthcare Bio-Sciences AB) with a 1/1 binding model.

Root growth assay

Seedlings were grown on 1/2 MS plates for 5 d afterward, 12 plants were transferred to new 1/2 MS plates lacking or supplemented with the indicated concentrations of (+)-PAO1 or ABA. The plates were scanned on a flatbed scanner after 7 d to measure the root growth using the Image software ImageJ version 1.48.

Notes and references

1. R. Finkelstein, *Arabidopsis Book*, 2013, **11**, e0166.

2. R. Sean, L. Pedro, R. Ruth and R. Suzanne, 2010.

3. Y. Ma, I. Szostkiewicz, A. Korte, D. Moes, Y. Yang, A. Christmann and E. Grill, *Science*, 2009, **324**, 1064–8.

4. S.-Y. Park, P. Fung, N. Nishimura, D. R. Jensen, H. Fujii, Y. Zhao, S. Lumba, J. Santiago, A. Rodrigues, T.-F. F. Chow, S. E. Alfred, D. Bonetta, R. Finkelstein, N. J. Provart, D. Desveaux, P. L. Rodriguez, P. McCourt, J.-K. Zhu, J. I. Schroeder, B. F. Volkman and S. R. Cutler, *Science*, 2009, 324, 1068–71.

5. K. Melcher, L.-M. Ng, X. E. Zhou, F.-F. Soon, Y. Xu, K. M. Suino-Powell, S.-Y. Park, J. J. Weiner, H. Fujii, V. Chinnusamy, A. Kovach, J. Li, Y. Wang, J. Li, F. C. Peterson, D. R. Jensen, E.-L. Yong, B. F. Volkman, S. R. Cutler, J.-K. Zhu and H. E. Xu, *Nature*, 2009, **462**, 602–8.

6. K.-I. Miyazono, T. Miyakawa, Y. Sawano, K. Kubota, H.-J. Kang, A. Asano, Y. Miyauchi, M. Takahashi, Y. Zhi, Y. Fujita, T. Yoshida, K.-S. Kodaira, K. Yamaguchi-Shinozaki and M. Tanokura, *Nature*, 2009, **462**, 609–14.

7. F. Vlad, S. Rubio, A. Rodrigues, C. Sirichandra, C. Belin, N. Robert, J. Leung, P. L. Rodriguez, C. Laurière and S. Merlot, *Plant Cell*, 2009, 21, 3170–84.

8. F.-F. Soon, L.-M. Ng, X. E. Zhou, G. M. West, A. Kovach, M. H. E. Tan, K. M. Suino-Powell, Y. He, Y. Xu, M. J. Chalmers, J. S. Brunzelle, H. Zhang, H. Yang, H. Jiang, J. Li, E.-L. Yong, S. Cutler, J.-K. Zhu, P. R. Griffin, K. Melcher and H. E. Xu, *Science*, 2012, 335, 85–8.

9. H. Fujii, V. Chinnusamy, A. Rodrigues, S. Rubio, R. Antoni, S.-Y. Park, S. R. Cutler, J. Sheen, P. L. Rodriguez and J.-K. Zhu, *Nature*, 2009, **462**, 660–4.

10. D. Huang, M. R. Jaradat, W. Wu, S. J. Ambrose, A. R. Ross, S. R. Abrams and A. J. Cutler, *Plant J.*, 2007, **50**, 414–28.

11. J. Santiago, F. Dupeux, K. Betz, R. Antoni, M. Gonzalez-Guzman, L. Rodriguez, J. A. Márquez and P. L. Rodriguez, *Plant Sci.*, 2012, **182**, 3–11.

12. D. Sun, H. Wang, M. Wu, J. Zang, F. Wu and C. Tian, *Biochem. Biophys. Res. Commun.*, 2012, 418, 122–7.

13. X. Zhang, L. Jiang, G. Wang, L. Yu, Q. Zhang, Q. Xin, W. Wu, Z. Gong and Z. Chen, *PLoS One*, 2013, **8**, e67477.

14. J. Takeuchi, M. Okamoto, T. Akiyama, T. Muto, S. Yajima, M. Sue, M. Seo, Y. Kanno, T. Kamo, A. Endo, E. Nambara, N. Hirai, T. Ohnishi, S. R. Cutler and Y. Todoroki, *Nat. Chem. Biol.*, 2014, **10**, 477–82.

15. Z. Wang and R. B. Silverman, *Bioorg. Med. Chem.*, 2006, **14**, 2242–52.

16. Y. Todoroki, K. Kobayashi, M. Shirakura, H. Aoyama, K. Takatori, H. Nimitkeatkai, M.-H. Jin, S. Hiramatsu, K. Ueno, S. Kondo, M. Mizutani and N. Hirai, *Bioorg. Med. Chem.*, 2009, **17**, 6620–30.

17. J. M. Nyangulu, K. M. Nelson, P. A. Rose, Y. Gai, M. Loewen, B. Lougheed, J. W. Quail, A. J. Cutler and S. R. Abrams, *Org. Biomol. Chem.*, 2006, **4**, 1400–12.

18. J. M. Nyangulu, M. M. Galka, A. Jadhav, Y. Gai, C. M. Graham, K. M. Nelson, A. J. Cutler, D. C. Taylor, G. M. Banowetz and S. R. Abrams, *J. Am. Chem. Soc.*, 2005, **127**, 1662–4.

19. C. Diedrich and S. Grimme, *J. Phys. Chem. A*, 2003, **107**, 2524–2539.

20. F. Dupeux, J. Santiago, K. Betz, J. Twycross, S.-Y. Park, L. Rodriguez, M. Gonzalez-Guzman, M. R. Jensen, N. Krasnogor, M. Blackledge, M. Holdsworth, S. R. Cutler, P. L. Rodriguez and J. A. Márquez, *EMBO J.*, 2011, **30**, 4171–84.

21. Q. Hao, P. Yin, W. Li, L. Wang, C. Yan, Z. Lin, J. Z. Wu, J. Wang, S. F. Yan and N. Yan, *Mol. Cell*, 2011, **42**, 662–72.

22. M. Gonzalez-Guzman, G. A. Pizzio, R. Antoni, F. Vera-Sirera, E. Merilo, G. W. Bassel, M. A. Fernández, M. J. Holdsworth, M. A. Perez-Amador, H. Kollist and P. L. Rodriguez, *Plant Cell*, 2012, **24**, 2483–96.

23. R. Antoni, M. Gonzalez-Guzman, L. Rodriguez, M. Peirats-Llobet, G. A. Pizzio, M. Fernandez, N. De Winne, G. De Jaeger, D. Dietrich, M. J. Bennett and P. L. Rodriguez, *Plant Physiol.*, 2012, **161**, 931–941.

24. M. Okamoto, F. C. Peterson, A. Defries, S.-Y. Park, A. Endo, E. Nambara, B. F. Volkman and S. R. Cutler, *Proc. Natl. Acad. Sci. U. S. A.*, 2013, **110**, 12132–7.

25. E. F. Pettersen, T. D. Goddard, C. C. Huang, G. S. Couch, D. M. Greenblatt, E. C. Meng and T. E. Ferrin, *J. Comput. Chem.*, 2004, **25**, 1605–12.

Figure legends

Fig. 1 Structure of ABA and its analogs

Fig. 2 Physiological effects of optical isomers of (+)-PAO4 compared with that of AS6. *Arabidopsis* seed germination rate in response to 0.3 μM ABA and (+)-PAO4 or AS6 applied when the germination rate of ABA-treated plants was 40% (n = 3; error bars represent s.d.).

Fig. 3 Effect of (+)-PAO4 on lettuce seed germination compared with that of AS6. Seed germination rate in the presence of 10 μM ABA and 30 or 300 μM (+)-PAO4 or AS6. Similar results were obtained in three independent experiments.

Fig. 4 Effect of (+)-PAO1 and (+)-PAO4 on HAB1 inhibition by ABA receptors compared with that of AS6. (a) Chemical inhibition of HAB1 by various ABA receptors in the presence of 10 μM of each test compound or (b) PYR1 and PYL5 in the presence of various concentrations (0, 0.05, 0.5, 1, 5, 10, 25, and 50 μM) of (+)-PAO4 or AS6. (c) Antagonistic effect of each test compound against various ABA receptors and (d) effect of (+)-PAO4 and AS6 on PYR1 and PYL5. Assays were performed in the presence of 5 μM ABA and (c) 50 μM of each compound or (d) various concentrations (0, 0.5, 25, 5, 10, 25, 50 and 50 μM) of (+)-PAO4 or AS6. HAB1 activity in the absence of receptor proteins and test compounds is expressed as 100% of enzyme activity. PYL and HAB1 proteins were used at the same molar ratio of 60 pmol (n=3; error bars represent s.d.).

Scheme 1 Synthesis of (±)-PAOn (n = 1–6).

Table 1 Apparent binding affinity of (+)-PAO1 and (+)-PAO4 for PYLs

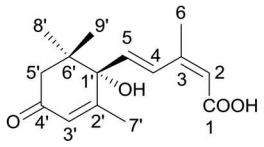

ABA (**1**)

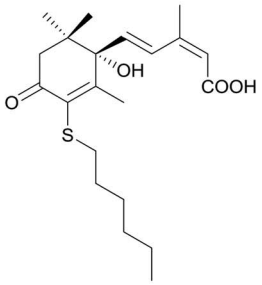

AS6 (**2**)

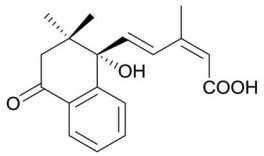

Tetralone ABA (**3**)

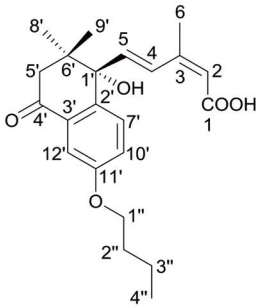

(+)-PAO4 (**4**)

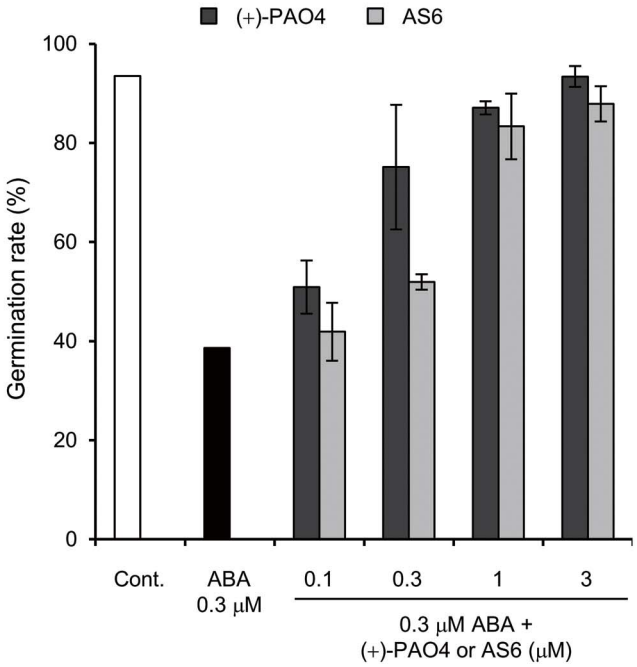
(+)-PAO4
AS6
Germination rate (%)
100
80
60
40
20
0
Cont.
ABA
0.3 μM
0.1
0.3
1
3
0.3 μM ABA +
(+)-PAO4 or AS6 (μM)

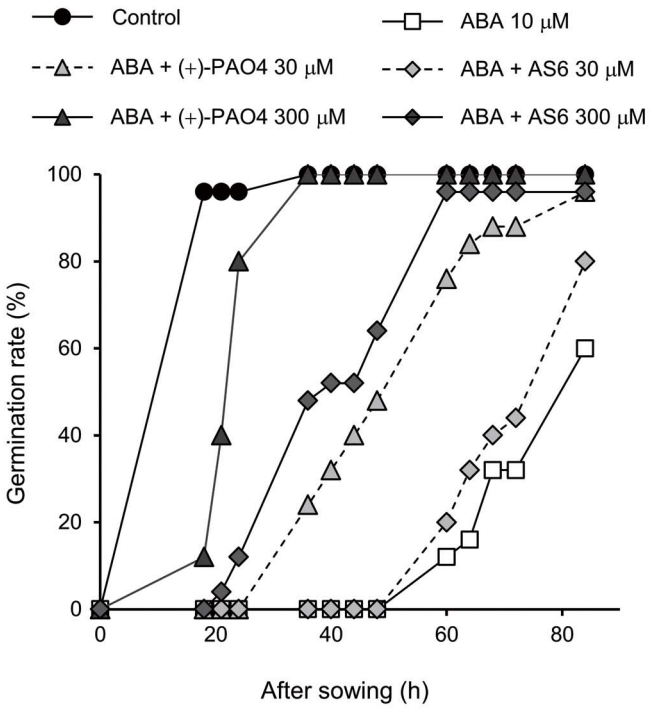
Control
ABA 10 μM
ABA + (+)-PAO4 30 μM
ABA + AS6 30 μM
ABA + (+)-PAO4 300 μM
ABA + AS6 300 μM
Germination rate (%)
100
80
60
40
20
0
0
20
40
60
80
After sowing (h)

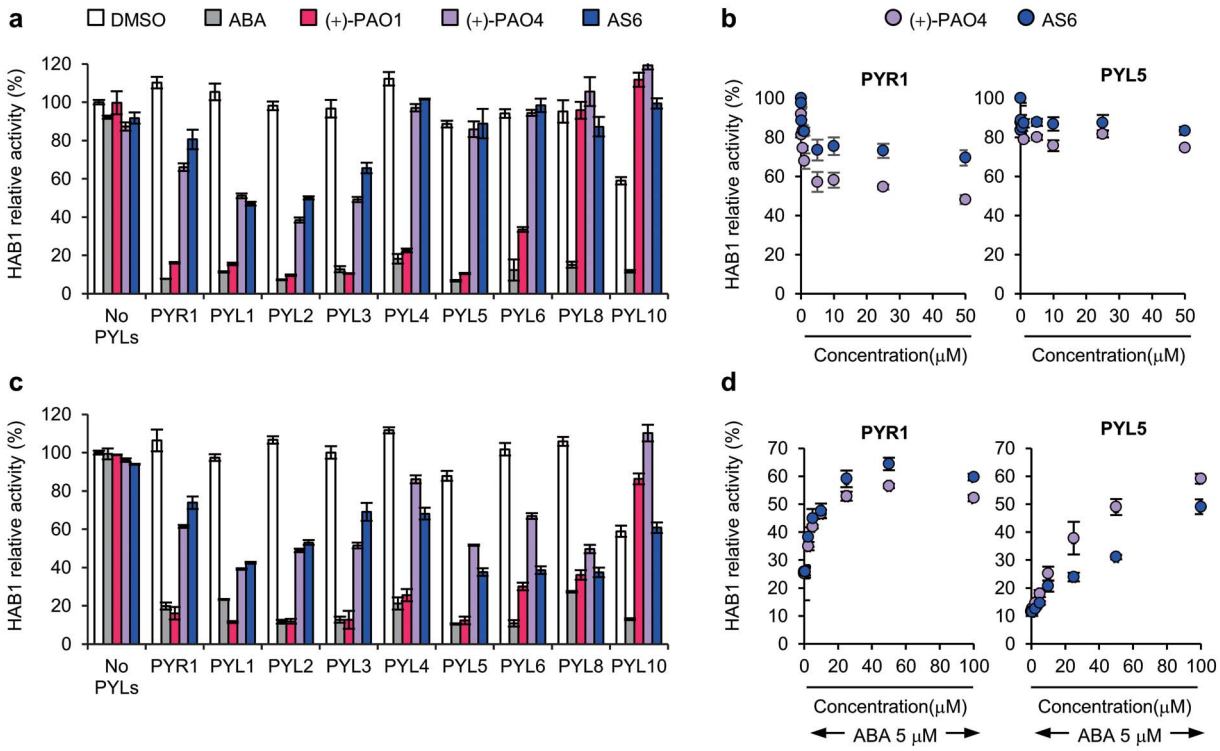
a
DMSO
ABA
(+)-PAO1
(+)-PAO4
AS6
HAB1 relative activity (%)
No PYLs
PYR1
PYL1
PYL2
PYL3
PYL4
PYL5
PYL6
PYL8
PYL10
b
(+)-PAO4
AS6
PYR1
PYL5
Concentration(μM)
c
d
ABA 5 μM

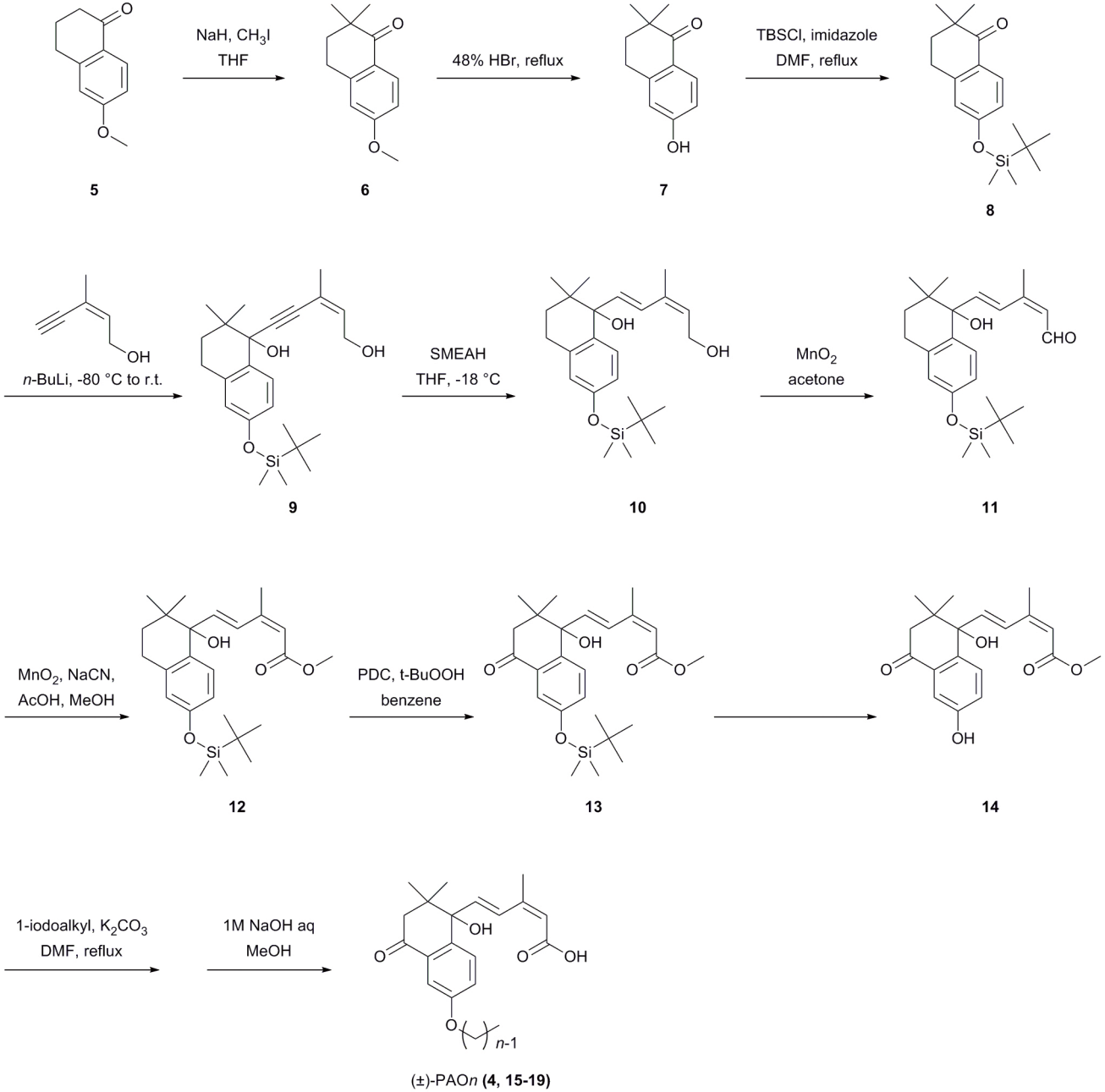
NaH, CH3I
THF
48% HBr, reflux
TBSCl, imidazole
DMF, reflux
5
6
7
8
n-BuLi, -80 °C to r.t.
SMEAH
THF, -18 °C
MnO2
acetone
9
10
11
MnO2, NaCN,
AcOH, MeOH
PDC, t-BuOOH
benzene
12
13
14
1-iodoalkyl, K2CO3
DMF, reflux
1M NaOH aq
MeOH
n-1
(±)-PAOn (4, 15-19)

Scheme 1

Table 1 Apparent binding affinity of (+)-PAO1 and (+)-PAO4 for PYLs[a]

Receptors	Compounds	K_d (μM)	ΔH (kcal/mol)	$-T\Delta S$[b] (kcal/mol)	ΔG[c] (kcal/mol)
PYL5	(+)-PAO1	0.20 ± 0.03	–6.3 ± 0.1	–2.7	–9.0 ± 0.1
PYL5	(+)-PAO4	0.13 ± 0.04	–6.7 ± 0.1	–2.6	–9.2 ± 0.2
PYL5	AS6	0.48 ± 0.10	–9.7 ± 0.2	1.2	–8.5 ± 0.1
PYL10	(+)-PAO1	2.19 ± 0.37	–10.3 ± 0.3	2.7	–7.6 ± 0.1
PYL10	(+)-PAO4	1.39 ± 0.23	–8.9 ± 0.2	2.0	–7.9 ± 0.1
PYL10	AS6	1.28 ± 0.72	–6.9 ± 0.5	–1.0	–7.9 ± 0.3

[a] K_d, ΔH obtained from single-set-of-sites fit to date.

[b] $T\Delta S = \Delta H - \Delta G$

[c] $\Delta G = -RTln(1/K_d)$. Uncertinties for K_d, ΔH, and ΔG calculated by curve fitting program of MicroCal Origin 7.0.